26th IMEKO TC4 International Symposium
24th International Workshop on ADC and DAC Modelling and Testing
IMEKO TC-4 2023
Pordenone, Italy / September 20-21, 2023

Teamwork of Simulations and Hall Sensor Measurements for the Design of Magnetic Sensor Systems

Thomas Schliesch[1], Thomas Lindner[2]

[1] *Max Baermann GmbH, Germany, t.schliesch@max-baermann.de*
[2] *Max Baermann GmbH, Germany, t.lindner@max-baermann.de*

Abstract – **New magnetic sensor systems like stray field compensating specimen demand new challenges for the design of respective permanent magnets and sensors themselves. The collaboration of FEM simulations with 3D-Hall sensor measurements provides new insights how to build and optimize such systems. The paper shows this by the example of two stray field compensating sensors for position detection of rotating systems. The first example provides different stages of the development of a new sensor. The second one shows steps during the improvement of permanent magnets for a commercially available sensor system. Both parts also supply results about the insensitivity of those sensors against external fields up to 20mT.**

I. INTRODUCTION

Magnetic sensors have become more and more complicated during the last decades. Since a few years sensors with compensation of external stray fields became of increased familiarity. Hall sensors doing this are mainly based on the gradient principle where pairs of Hall sensor signals are evaluated and often these sensors consist of arrays of those units. The design of adequate magnets and their impact on those sensors on one hand can be done with numerical simulations of respective magnets. The input to the single sensor elements can be taken from the simulation results. On the other hand, the viability of a combination of single sensor signals for an adequate output of the whole sensor, like e.g. an angle of rotation, should be proved by measurements before investing into hardware. This can be done with devices for 3D Hall sensor measurements and there by combining the single signals to an output similar to that of the aimed final sensor.

The paper will show one example how the combination of simulations, Hall sensor measurements as well the final hardware realization had been done for an external field compensating sensor. This sensor can be used for on-axis as well as for off-axis rotating systems.

Another example refers to a commercially available sensor system where a magnet had to be optimized to provide position information of high accuracy and low noise to signal ratio. The magnet had to be improved with respect to the magnetization pattern as well as with respect to its final shape. Simulation results had to be surveyed by surface mapping of fastidious combinations of field gradients. Further the stray field stability of the final sensor system had to be checked.

II. GRADIENT SENSOR FOR CYLINDRIC MAGNETS WITH AXIAL POLARIZATION

The idea of this sensor was to harvest the radial field components of axially magnetized cylinder magnets at locations, where a mutual movement of magnet and sensor would not alter the field gradient. Fig. 1 shows the simulated distribution of the axial component of remanence of a bow shaped magnetized ring magnet with outer diameter 30mm, inner diameter 16mm, axial length 5mm and with four poles. Magnet material is injection molded isotropic NdFeB here. Magnets like this can provide nearly constancy and large steepness of the radial field component above the magnet's head face. For the one of Fig. 1 the radial field gradient is higher than 30mT/mm at 1.5mm axial distance.

The constant field gradient and the sinusoidal field dependence in angular direction led to the idea to design a sine-cosine sensor by using sensor pairs with adequate phase distance here of $\pi/4$ for the four-pole magnet, which can be generalized to other pole numbers, [1]. Fig. 2 displays the backside of an experimental sensor board, which was finally assembled in a research project with the INNOVENT institute, [2]. The single sensors within one pair had a radial distance of 2.5mm each.

The experimental prove of concept was made with a 3D-Hall measurement device according to Fig. 3 on various magnetic and non-magnetic shafts. Prior to that the same was performed with FEM simulations by combination of single signals on different paths along the magnet.

External fields to proof the stability against external stray fields were applied by permanent magnets as can also be seen in Fig. 3 on the right side.

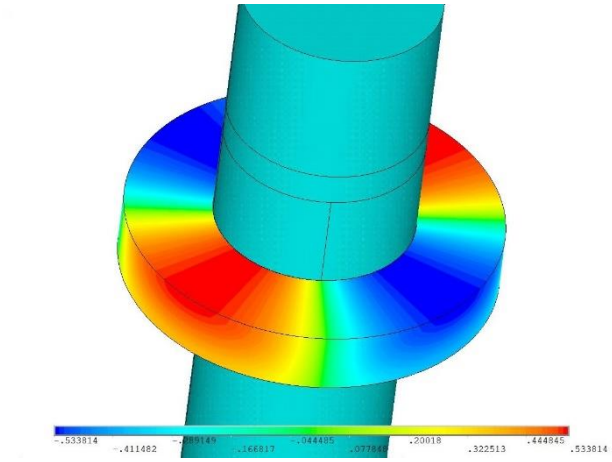

Fig. 1: FEM model of an injection molded NdFeB magnet with axially bow shaped polarization.

Fig. 2: Backside of circuit board of the sensor with two radial Hall-sensor pairs assembled by INNOVENT, [2].

Table 1: Average angular error amplitudes simulated by Hall probe measurements according to Fig. 3

Material	0mT	9mT	0mT	9mT
	non-magnetic shaft		soft magnetic shaft	
Ferrite	5.1	5.7	4.4	5.4
NdFeB	3.1	3.3	2.9	3.5

In Table 1 the simulated results by Hall probe measurements according to Fig. 3 are summarized for two materials. Beside the mentioned isotropic NdFeB magnets with bow shaped polarization in addition anisotropic Ferrite magnets with rigid four pole magnetization were investigated. Measurements were done with non-magnetic as well as with soft magnetic shafts.

Fig.4 provides results for a Ferrite magnet investigated with the real sensor according to Fig. 2. Here stray fields up to 20mT were applied by using respective Helmholtz-coils. As can be seen from Table 1 and from Fig. 4 the stray field resistance could be proven. What was less satisfying are the relatively large angular errors. Those originated mainly from the field shapes of the magnets.

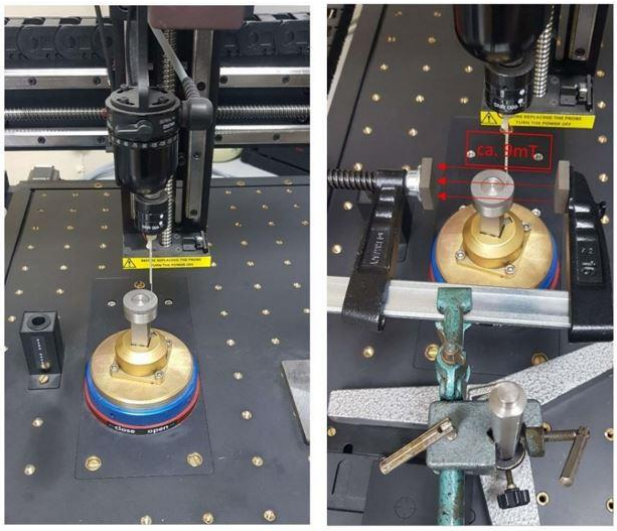

Fig. 3: 3D Hall-measurements and the application of external fields by permanent magnets, [3].

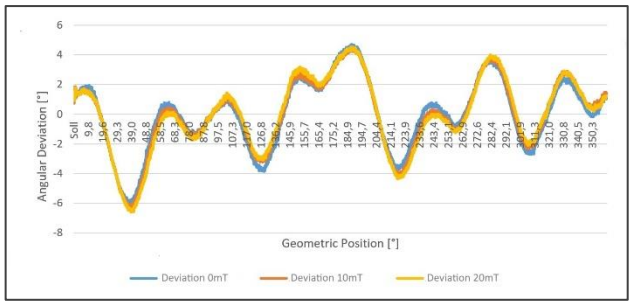

Fig. 4: Angular errors of the final sensor system for a Ferrite magnet at different external fields. Investigations on non-magnetic shaft.

The deviation from a sinus shape of the Ferrite magnet was obvious by the rigid pole pattern with homogeneous magnetization within each pole. But deviations from a sinus magnetization also occurred at the NdFeB magnets due to a non-adequate magnetizing coil. This led to an idea to develop a concept for a sensor to compensate at least partially the higher harmonics in the magnets' signals. The scheme for this, again for a gradient sensor similar to the one above, is provided by Fig.5. Here a combination of different field components as well as again the calculation of differences within the sensor pairs have to be performed.

For the same magnets as discussed above now axial and tangential field components are harvested. The evaluation of the signals of the two new field components were done now at radii more closely to the outer radius of the magnet. Further the axial distance to the head face was raised.

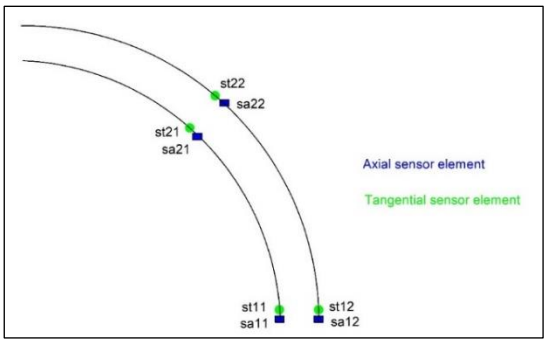

Fig. 5: Sensor concept with partial compensation of higher harmonics as well as of external fields.

Eq. (1)-(3) provide the related scheme of the functionality of the new concept:

$$\begin{aligned} \Delta a_1 &= sa_{12} - sa_{11} \\ \Delta a_2 &= sa_{22} - sa_{21} \\ \Delta t_1 &= st_{12} - st_{11} \\ \Delta t_2 &= st_{22} - st_{21} \end{aligned} \tag{1}$$

After calculating difference signals sine and cosine parts are calculated in the way according to eq. (2). The scheme can be understood by the fact, that in most cases both field components have similar higher harmonics by strength but with opposite sign:

$$\begin{aligned} B_{sin} &= \Delta a_1 + \Delta t_2 \\ B_{cos} &= \Delta a_2 - \Delta t_1 \end{aligned} \tag{2}$$

Finally, we get for the angle of rotation α where n_p is the number of poles:

$$\alpha = \frac{2}{np} \arctan\left(\frac{B_{sin}}{B_{cos}}\right) + \alpha_0 \tag{3}$$

In Fig. 6 the sensor simulation by the 3D-Hall measurement is displayed for a sintered Ferrite magnet. At the top left the single fields are shown at both angular positions, but for clarity only at one radius. One can see clearly that there are large deviations from a sinusoidal shape. The top right picture provides the differences according to eq. (1). The bottom left reveals, that by the concept of eq. (2) a much more viable shape exists, and the bottom right provides the angular error. Here with a non-magnetic shaft the average error amplitude of the Ferrite magnet is much smaller compared to that of the first other sensor, compare to table 1. Similar results exist for the NdFeb-magnets, where the angular errors were reduced by more than 50%.

The sensor principle of Fig. 5 can be used for on-axis and an off-axis systems and can also be used for systems harvesting a radial instead of an axial field component. A respective hardware version of this system has not been built yet, [4].

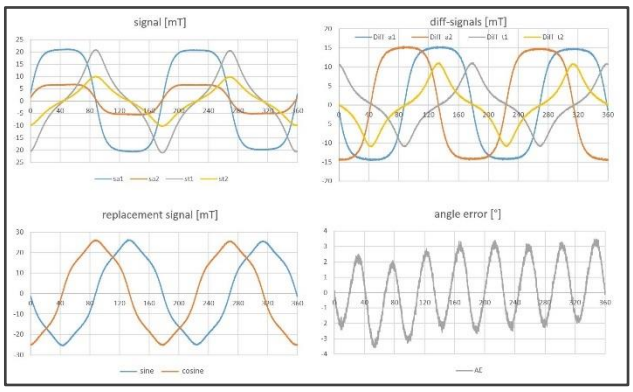

Fig. 6: Simulation of a new sensor concept according to Fig. 5 with 3D-Hall measurements for an anisotropic Ferrite magnet.

III. IMPROVED MAGNETS FOR AN ON-AXIS STRAY FILD IMMUNE SENOR

A sensor which harvests mainly the in-plane components of fields perpendicularly to the axis of a rotating shaft is described in [5] and [6]. Here an array of sensor pairs grouped circularly around the sensor center builds up a final sine-cosine system. The task related to this was to develop and optimize adequate magnets, to prove stray field immunity and to devise a practical system for quality control.

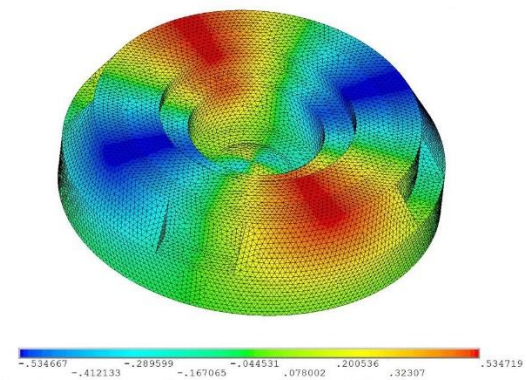

Fig. 7: FEM Analysis results for an on-axis sensor magnet for a stray field immune sensor system, axial component of remanence. Magnet diameter 14mm.

Fig. 7 displays the results of an FEM simulation of a respective magnet. The specimen shown here is made up of injection molded NdFeB with four poles on its head face. The sensor is mainly located at the center of rotation, but there can be eccentricities by mechanical tolerance up to 1.5mm. The bulge in the magnet's

center was devised to increase the space for the melt flow during the injection molding process.

Fig. 8 provides FEM-calculated results by adapting the receipt being described [6] to calculate the angular deviations at 1.5mm radius for two sorts of magnets. Axial distances to the magnet were 1.5 and 2.9mm. According to [6] sensor angles can be calculated by partial derivatives of in-plane field components. The rippled curves belong to full inherent analyses of the sensor.

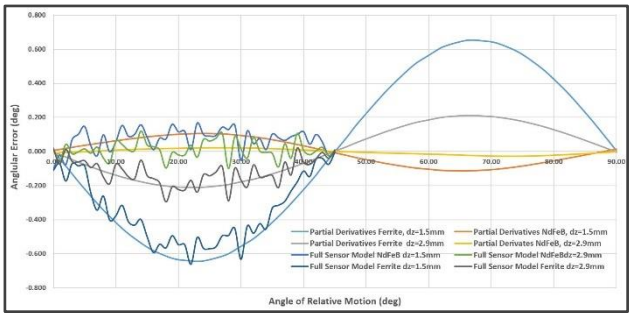

Fig. 8: FEM-calculated angular errors for a quarter of a full sensor path, magnets with geometry as in Fig. 7.

The curves with larger angular errors belong to injection molded Ferrite magnets with uniform direction of polarization within each pole. Fig. 9 displays stray field immunity investigations for such a magnet at radial positions 0mm and 1.3mm and at 1.5mm axial distance, using the real sensor. One can see that the results at the eccentricity position are in approximate agreement with the FEM predictions. On the other hand, a stray field immunity up to 10mT was proven.

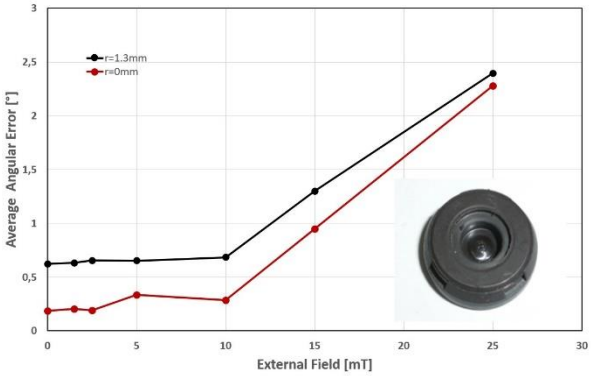

Fig. 9: Stray field immunity of real sensor with injection molded Ferrite with rigid magnetization.

The curves with the much lower angular errors in Fig.8 belong to NdFeB magnets with bow shaped magnetization. According to that, also injection molded, cost effective Ferrite magnets with bow shaped in mold-magnetization were manufactured. Their reduction of angular error could also be verified by real sensor measurements.

According to [6] for a reasonably low noise to signal ratio the parameter dB_{xy}/dxy as being defined in eq. (4) must be larger than 8mT/mm. For the Ferrite specimen it could be reached well by mainly keeping the bore radius inside the specimen as low as possible.

$$\frac{dB_{xy}}{dxy} = \frac{1}{2} \cdot \sqrt{\left(\frac{\partial B_y}{\partial x} + \frac{\partial B_x}{\partial y}\right)^2 + \left(\frac{\partial B_y}{\partial y} - \frac{\partial B_x}{\partial x}\right)^2} \qquad (4)$$

Fig. 10 displays the results of dB_{xy}/dxy above a Ferrite magnet with decreased inner diameter at dz=1.5mm. They were measured by a device according to Fig. 3, utilizing again a 3D Hall sensor. The limit of 8mT/mm is surpassed by far. The results are in excellent agreement with FEM simulations.

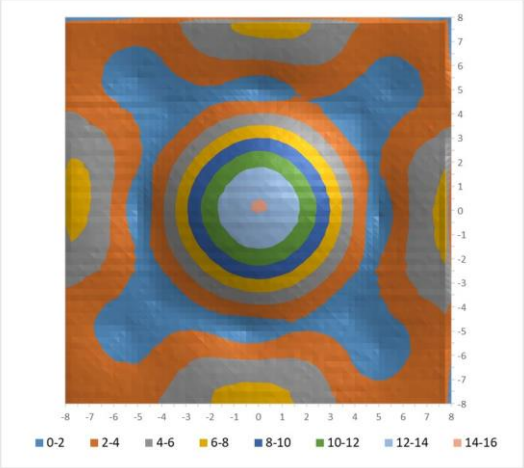

Fig. 10: dB_{xy}/dxy for a Ferrite magnet with decreased bore radius and bow-shaped polarization.

REFERENCES

[1] T.Schliesch, Hall Sensor, WO 2016/166265 A1, Max Baermann GmbH.

[2] Magnetic Off-Axis Sensor System for Control of Rotating Movements – RoCo, AIF Research Project, Germany 2021, Grant KK5209101DH1.

[3] Senis AG, Magnetic Field Mapper MMS-1A-RS.

[4] T.Schliesch, Method to Detect a Relative Angular Position and Magnetic Encoder Device, Patent Pending, 2022.

[5] C.Schott, S.Huber, Arrangement, Method and Sensor for Measuring an Absolute Angular Position Using a Multipole Magnet, WO 2014/029885 A1, Melexis Technologies NV.

[6] Magnet Selection for MLX9037X-Rotary Stray-Field Immune Mode, Application Note, Melexis Technologies NV, 2017.